Forest Ecology and Management 585 (2025) 122497

Contents lists available at ScienceDirect

Forest Ecology and Management

journal homepage: www.elsevier.com/locate/foreco

An integrated approach combining bi-temporal airborne laser scanning and X-ray microdensitometry in assessing wood properties

Maryam Poorazimy [a,*], Ghasem Ronoud [a], Tuomas Yrttimaa [a], Juha Hyyppä [b], Ninni Saarinen [a], Ville Kankare [c], Mikko Vastaranta [a]

[a] School of Forest Sciences, University of Eastern Finland, Joensuu 80101, Finland
[b] Department of Photogrammetry and Remote Sensing, Finnish Geospatial Research Institute, National Land Survey of Finland, Espoo 02150, Finland
[c] Department of Geography and Geology, University of Turku, Turku 20014, Finland

ARTICLE INFO

Keywords:
Wood density (WD)
Ring width (RW)
Tree Growth
Norway spruce
Scots pine

ABSTRACT

Information on wood properties across trees and stands is needed to support silviculture and wood procurement. Wood properties of standing trees are usually measured by destructive sampling limiting the number of observations that can be collected across a range of forest structural and environmental conditions. In contrast, airborne laser scanning (ALS), with its capability to characterize tree crowns and their increment over time, could provide a non-destructive approach for assessing wood properties. This study aimed at relating ALS-derived mean annual increments in tree height and crown dimensions between 2009 (T1) and 2023 (T2) to X-ray microdensitometry-measured mean ring width ($RW_{mean\text{-}tree}$) and basal-area weighted mean wood density ($WD_{mean\text{-}tree}$) formed during the same period. The experimental design comprised 257 Scots pines (*Pinus sylvestris* L.) and 142 Norway spruces (*Picea abies* (L.) Karst.) across 59 sample plots representing varying boreal forest conditions. As per our investigations, the mean annual increment in tree height (ΔH_{mean_tree}) represented the strongest correlations with RW_{mean_tree} for both tree species ($r = 0.43$–0.44) and a weak but statistically significant correlation with WD_{mean_tree} for Norway spruces only ($r = -0.17$). When aggregating individual tree observations for plot-level, ΔH_{mean_plot} exhibited moderate correlations ($r = 0.47$–0.48) with RW_{mean_plot} for both species. WD_{mean_plot} of Scots pines showed a correlation of 0.36 with the averaged mean annual increments of crown surface area. However, none of the metrics were significant for WD_{mean_plot} of Norway spruces. By utilizing the linear-mixed effect model 40–41 % of the variations in RW_{mean_tree} of Scots pines and Norway spruces could be explained when accounting for the variability between sample plots. Based on our study, it appears that some of the variation in wood properties, particularly in ring width, can be captured using bi-temporal ALS measurements. However, assessing wood properties over large areas remains challenging and requires further research.

1. Introduction

Information on wood properties is essential for supporting decision-making in forestry (Wylie et al., 2019). Wood density (WD) is among the wood properties that directly affect tree biomass and carbon content (Demol et al., 2021; Pokharel et al., 2016; Van Leeuwen et al., 2011). Moreover, the stiffness of wood is governed by wood density and its variation from pith to bark and bottom to top, with microfibril angle playing a significant role (Demol et al., 2021; Van Leeuwen et al., 2011). Another wood property affecting the physical and chemical characteristics of timber is ring width (RW) (Van Leeuwen et al., 2011). It is considered crucial in dendrochronology and growth patterns studies (Genet et al., 2013; Zeller et al., 2017; Ahmed et al., 2024; Jevšenak et al., 2024).

Nowadays, wood properties can be measured using X-ray microdensitometry systems such as SilvaScan™ or ITRAX (Downes and Drew, 2008; Peltola et al., 2007; Schimleck et al., 2019). However, these methods are expensive and labor-intensive as the wood samples need to be taken whereas information on wood properties across a broad range of stands is needed for forest managers and mill owners (Van Leeuwen et al., 2011). Wood properties in general are known to vary by species, tree, stand, and site conditions. At the tree level, intrinsic features like

* Corresponding author.
E-mail address: maryam.poorazimy@uef.fi (M. Poorazimy).

https://doi.org/10.1016/j.foreco.2025.122497
Received 12 June 2024; Received in revised form 4 January 2025; Accepted 6 January 2025
Available online 18 March 2025

cambial age, WD, and RW, and the extrinsic ones including the tree height and crown dimensions as well as the size and placement of knots and branches influence wood properties (Duchesne et al., 1997; Krajnc et al., 2019; Kuprevicius et al., 2013; Mäkinen and Colin, 1998). At a broader scale, factors like competition, stocking density, and site conditions play a key role in determining wood properties (Ikonen et al., 2008; Kankare et al., 2022). Wood properties also change over time due to tree and stand development, branch mortality, and branch wound occlusion (Hein et al., 2008; Van Leeuwen et al., 2011).

Tree crown structure, one of the mentioned indicators, refers to how branches are arranged along the stem. This affects the suitability of wood for different products, based on the number and features of knots in the timber. Hence, information on tree crowns has been widely used in modeling wood formation and predicting wood quality (Van Leeuwen et al., 2011). For example, according to Larson's (1969) conceptual model, trees with large crowns are likely to produce wood with poorer mechanical properties, as auxin produced in the stem apex shapes xylem characteristics, including cell size, wall thickness, and the ratio of earlywood to latewood. Mechanical loading of the crown that redistributes the growth to the region of high stress is another factor affecting xylem properties (Krajnc et al., 2019). Moreover, the crown and its increment over time have been shown as a determining indicator for predicting stem growth (Poorazimy et al., 2024; Pretzsch, 2021; Seidel et al., 2015; Yrttimaa et al., 2022). However, wood properties have been predicted using simple measures such as tree diameter at breast height (dbh), height, and age (Van Leeuwen et al., 2011). Even though tree size and age can be measured in the field, it is not possible to obtain these attributes for all trees across large areas, yet this information could support forest management and improve understanding of how wood properties vary over wide regions.

The emergence of laser scanning has enabled detailed measurements of the structural characteristics of trees and forest stands (Hyyppä et al., 2008; Kankare et al., 2014; Liang et al., 2016, Fassnacht et al., 2024). Airborne laser scanning (ALS), collected via aircraft or drones flying over forested landscapes, captures data such as tree heights, crown dimensions, and the respective changes in these attributes over time if data acquisition is repeated (Duncanson and Dubayah, 2018; Frew et al., 2016; Ma et al., 2018; Poorazimy et al., 2022). Terrestrial laser scanning (TLS) is typically collected from sample plots or stands, allowing for even more detailed measurements, such as the quantification of tree architecture, including branch dimensions, lengths, and angles (Åkerblom and Kaitaniemi, 2021; Raumonen et al., 2013). When TLS measurements are repeated, even millimeter-level changes, particularly at the stem, can be detected (Luoma et al., 2021; Yrttimaa et al., 2023). Due to these precise capabilities, TLS has been used to assess various structural properties of trees, which are linked to wood characteristics and the quality of wood in the forest industry. For example, Pyörälä et al. (2019) compared standing tree log geometry from TLS to their measurements in the sawmill which was cut to length according to the specific bucking matrix as well as wood properties measured by X-ray scanning including WD and knottiness. In a recent study, Kankare et al. (2022) used TLS to evaluate dependencies of Scots Pine (*Pinus sylvestris* L.) structure and competitional status with wood properties of WD and RW in the southern boreal forest. However, as mentioned, TLS can only cover small, localized areas due to the need to frequently reposition the scanner, as observations from a single scanning location are limited to trees and tree parts that are within the scanner's line of sight (Liang et al., 2016). Therefore, to predict wood properties across large, forested regions for supporting silviculture, forest management, and the understanding of wood property variability, ALS appears more appealing (White et al., 2017). In addition, ALS is widely used for forest mapping in many countries where forestry is among the key industries (White et al., 2016). In such regions, ALS datasets are often openly provided by governments, and there are regular ALS acquisition programs in place, ensuring the continued availability of data in the future. Several countries aim for a 5- to 10-year cycle in ALS data collection, which offers unique opportunities to use this data for a better understanding of forest growth and to link forest growth metrics with wood properties (Fassnacht et al., 2024).

Hence, the study aimed to investigate how changes in tree height and crown dimensions acquired with bi-temporal ALS can be linked with wood properties obtained with an X-ray microdensitometry. We studied how the relationship differed between Scots pine and Norway spruce (*Picea abies* L. Karst.) at both individual tree and plot levels during the study period from 2009 (T1) to 2023 (T2). Investigated wood properties included the basal area-weighted mean WD (WD_{mean_tree}) and mean RW (RW_{mean_tree}) of individual trees measured between T1 and T2 as well as their means (WD_{mean_plot}, RW_{mean_plot}) and standard deviations (WD_{std_plot}, RW_{std_plot}) aggregated for each sample plot. ALS data were also processed to characterize mean annual increments of individual trees in height (ΔH_{mean_tree}) and crown dimensions (ΔC_{mean_tree}) between T1 and T2 as well as their means (ΔH_{mean_plot}, ΔC_{mean_plot}) and standard deviations (ΔH_{std_plot}, ΔC_{std_plot}) for each sample plot. With these investigations, we aimed to assess the feasibility of an approach relating ALS-derived growth metrics to wood properties, emphasizing the use of bi-temporal datasets to support forest management, forest planning, and wood procurement.

2. Materials and methods

2.1. Study area and sample plots

The study area was located in the southern boreal forest of Finland, Evo, bounded by 61°19.6′ N and 25°10.8′ E (Fig. 1). The experiment consisted of 59 sample plots, each measuring 32 × 32 m, established in 2014. These plots were dominated by Scots pine (*Pinus sylvestris* L.) and Norway spruce (*Picea abies* (L.) Karst.) with a mixture of birch (*Betula* sp.) and aspen (*Populus tremula* L.) trees. Tree-wise inventory, measuring dbh with a caliper, height with a Vertex IV clinometer, and determining species and health status through visual interpretation, was conducted for trees exceeding the dbh threshold (5 cm) during the field measurements in 2014 (Table 1).

2.2. Wood sampling and X-ray microdensitometry measurements

Identified trees in the field measurements in 2014 were considered as the population for sampling. Wood samples were collected only for Scots pine and Norway spruce trees using an increment borer at a fixed height of 1.30 m above the ground in April-May 2023 (Fig. 2).

The selection of sample trees per plot was carried out for the trees that are located within an 11-meter distance from the plot center and have a height of more than 80 % of the dominant height in that plot, to enhance the likelihood of detecting these sample trees in the ALS data. In addition, sample trees were distributed between dbh classes and the plot sectors spanning 90° with the main cardinal point at the middle of each, presenting various trees and stand conditions. Overall, 273 Scots pine and 150 Norway spruce wood samples were collected. The structural characteristics of sample trees have been provided in Table 2.

The ITRAX X-ray microdensitometry system was used for generating WD profiles for each sampled tree, representing WD and RW of the sampled tree rings (Cox Analytical Systems, Göteborg, Sweden). First, the air-dried samples with a 12 % moisture content were scanned in the batch mode and standard X-ray intensity in an exposure time of 20 ms (Peltola et al., 2007), generating digital radiographic images with horizontal and vertical pixel sizes of 25 μm. Second, WD profiles were obtained from scanned images using density software (Bergsten et al., 2001). It was further analyzed to calculate the sample trees mean WD (WD_{mean_tree}) and RW (RW_{mean_tree}) aligning with ALS acquisitions (Section 2.3). Since wood sampling took place in April-May 2023, WD_{mean_tree} and the RW_{mean_tree} were computed based on tree rings corresponding years 2009–2022 while omitting the possible early season of 2023 (i.e., not representing an entire growing season) to maintain

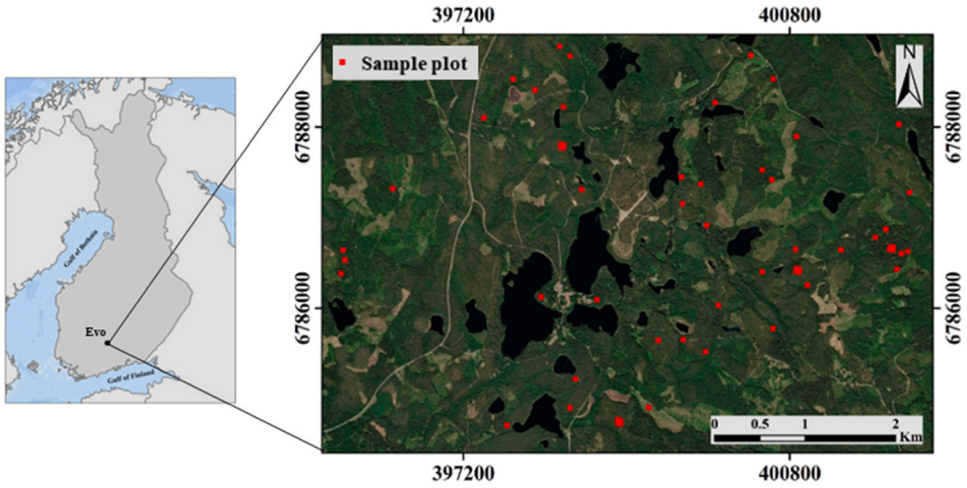

Fig. 1. Study area in Evo, Finland, and distribution of sample plots over Esri's world imagery basemap.

Table 1
Descriptive statistics of sample plot measurements (n = 59) in 2014 including minimum (Min), maximum (Max), mean, and standard deviation (Std.).

Attribute	Min	Max	Mean	Std.
Number of trees (n/ha)	342	3076	820	485
Mean volume (m^3/ha)	49.44	518.39	280.91	119.57
Basal area-weighted mean dbh (cm)	14.81	46.42	26.71	7.50
Basal area-weighted mean height (m)	12.70	31.09	21.75	4.61

the consistency of the measurements. WD_{mean_tree} was weighted by basal area, meaning it was computed as a weighted average across the sampled rings with the WD of each ring weighted according to its basal area derived from ring width measurements (Biondi and Qeadan, 2008). To obtain plot-level measures for mean wood properties by species, the tree-level measures were averaged (WD_{mean_plot}, RW_{mean_plot}). Additionally, their standard deviations (WD_{std_plot}, RW_{std_plot}) were calculated for sample plots with at least three observations per species. Table 2 summarizes the variability of these attributes across the sample plots.

2.3. Bi-temporal ALS data acquisition and characterizing tree crown dimensions

Bi-temporal ALS data covering the sample plots were used in this study. T1 ALS was collected in 2009 using a Leica ALS50-II SN058 scanner mounted on an airplane, providing an average point density of 25 pts/m^2. For T2 ALS data acquisition in 2023, a helicopter-borne Riegl VUX-1HA scanner was utilized to provide an average of 1182 pts/m^2 point density. Table 3 summarizes the acquisition parameters of these datasets.

All ALS data were first clipped by sample plot boundaries utilizing a 5 m buffer around each plot to ensure that all relevant trees become reconstructed. Ground points were distinguished from non-ground points using LAStools software (rapidlasso GmbH, Austria). It uses variations on a progressive densification filter algorithm based on triangulation of the lowest points considered to represent ground surface level (Axelsson, 2000). Then, point cloud elevations were normalized to heights above the ground surface by subtracting the corresponding ground height from the Z coordinates. Then, canopy height models

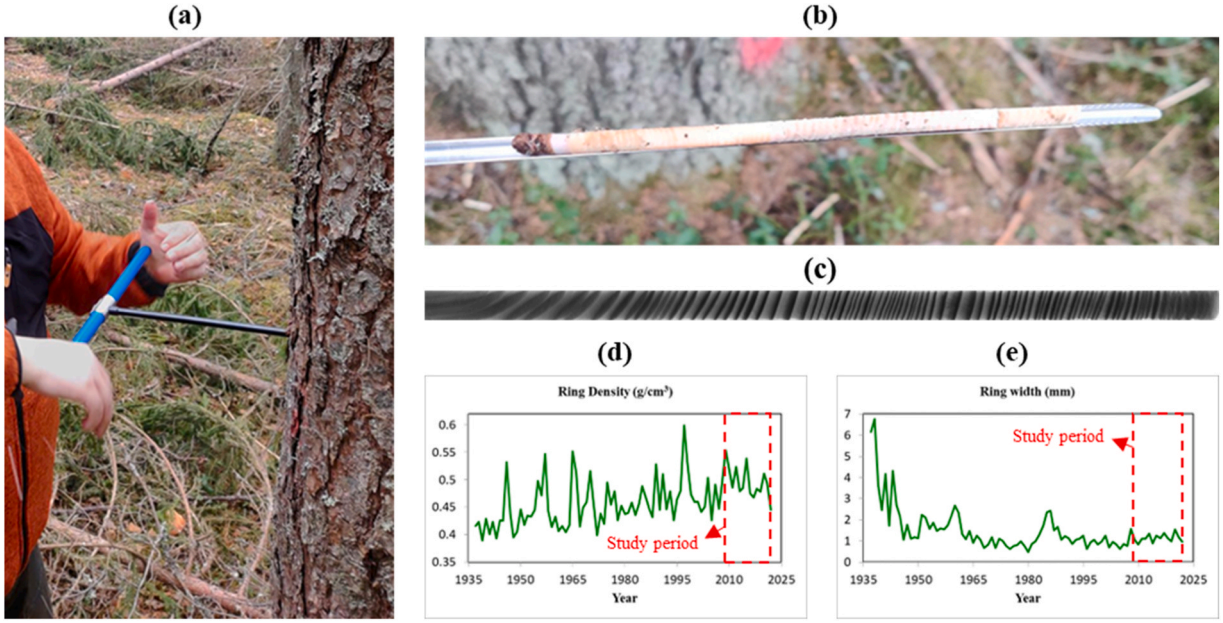

Fig. 2. Wood sampling using an increment borer (a) and the core extracted from the tree (b), the digital radiographic image generated by X-ray microdensitometry (c), and the resulting wood density (d) and ring width (e) profiles spanning the tree's lifetime. The red dashed line represents the study period.

Table 2
Field-measured sample tree structural characteristics of diameter at breast height (dbh), height (h), stem volume (v), and age in 2014, and X-ray microdensitometry measurements including 1) basal area weighted mean wood density (WD_{mean_tree}) and mean ring width (RW_{mean_tree}) between T1 (2009) and T2 (2023) and 2) their plot-level means (WD_{mean_plot}, RW_{mean_plot}) as well as standard deviations (WD_{std_plot}, RW_{std_plot}). Minimum (Min), maximum (Max), mean, and standard deviation (Std.) are presented.

	Min	Max	Mean	Std.
	Tree-level statistic of Scots Pine/Norway spruce sample trees (n = 273/150)			
dbh (cm)	9.45/5.95	63.00/57.90	25.02/29.40	7.45/9.12
h (m)	11.70/5.80	35.50/36.60	20.81/25.01	4.58/5.38
v (m^3)	0.05/0.01	4.30/3.39	0.57/0.93	0.54/0.63
Age (year)	28/28	175/173	64.40/84.40	32.50/31.95
WD_{mean_tree} (g/cm^3)	0.42/0.34	0.69/0.57	0.54/0.45	0.05/0.05
RW_{mean_tree} (mm)	0.28/0.28	2.53/3.18	1.26/1.24	0.46/0.51
	Statistics of the mean values of Scots Pine/Norway spruce dominated sample plots (n = 45/25)			
WD_{mean_plot} (g/cm^3)	0.44/0.40	0.60/0.49	0.54/0.45	0.03/0.02
RW_{mean_plot} (mm)	0.43/0.50	2.44/2.06	1.25/1.26	0.37/0.41
	Statistics of the standard deviation values of Scots Pine/Norway spruce dominated sample plots (n = 39/23)			
WD_{std_plot} (g/cm^3)	0.01/0.02	0.09/0.08	0.04/0.05	0.02/0.02
RW_{std_plot} (mm)	0.04/0.10	0.62/0.86	0.33/0.37	0.13/0.18

(CHMs) were created for both time points at a 0.5 m resolution by utilizing the pit-free algorithm originally developed by Khosravipour et al. (2016). The local maxima filter (LMF) with a fixed window size of 3 by 3 was employed to detect individual treetops. Those were considered markers in the marker-controlled watershed algorithm to eventually segment CHMs into tree crowns (Meyer and Beucher, 1990). After that, points located inside each tree crown segment were extracted and treated as individual tree point clouds. Points above a 2-m height threshold were considered to represent tree crowns and were further used for tree crown characterization (Fig. 3). For each tree, a 2D convex hull enveloping the crown points projected onto the XY plane was used to derive crown diameter (CD) and crown projection area (CA), whereas crown volume (CV) and crown surface area (CSA) were derived based on the volumetric characteristics of a respective 3D convex hull. Tree height (H) was determined as the highest point return within the crown segment. An illustration of the crown dynamic over time for a specific tree is provided in Fig. 3.

2.4. Tree-to-tree matching and calculating crown increments

To calculate the increments in tree height and crown dimensions and to investigate wood properties at individual tree and plot levels, tree-to-tree matching was applied. First, ALS-detected trees at T1 were matched with the closest ALS-detected trees at T2 within a maximum distance of

Table 3
Acquisition parameters of bi-temporal ALS data in years 2009 (T1) and 2023 (T2).

Year	Sensor	Field of view (°)	Wavelength (nm)	Laser pulse frequency (kHz)	Beam divergence (mrad)	Flying height (m)
2009 (T1)	Leica ALS50-II SN058	30	1064	150	0.22	400
2023 (T2)	Riegl VUX−1HA	360	1550	119	0.50	100

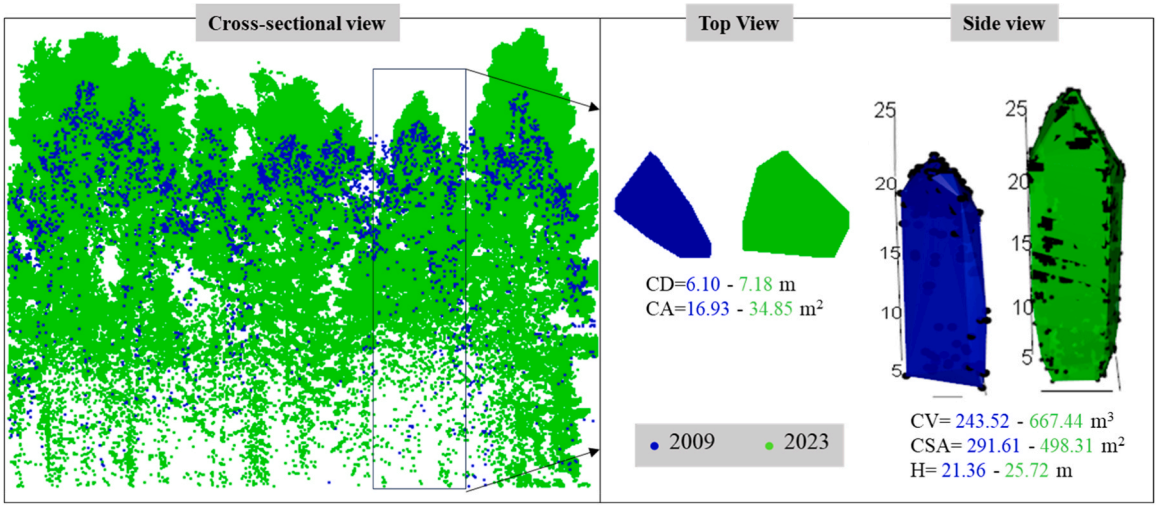

Fig. 3. A cross-sectional view of ALS point clouds depicting individual trees in 2009 (T1) and 2023 (T2) along a transect (left) as well as respective crown measures for a specific tree highlighted in a border from both top and side views (right). CD stands for crown diameter, CA for crown projection area, CV for crown volume, CSA for crown surface area, and H for tree height.

Table 4
Summary statistics for 1) the individual tree's mean annual increment in tree height and crown dimensions derived from bi-temporal ALS data between T1 (2009) and T2 (2023) (ΔH_{mean_tree}, ΔC_{mean_tree}) and 2) their means (ΔH_{mean_plot}, ΔC_{mean_plot}) and standard deviations (ΔH_{std_plot}, ΔC_{std_plot}) at plot-level. ΔH and ΔC stand for mean annual increments in tree height (H) and crown dimensions of diameter (CD), projection area (CA), volume (CV), and surface area (CSA). Minimum (Min), maximum (Max), mean, and standard deviation (Std.) are presented.

	Min	Max	Mean	Std.
	Tree-level statistics of Scots pine/Norway spruce sample trees (n = 257/142)			
ΔCD_{mean_tree} (m)	−0.15/−0.15	0.47/0.37	0.07/0.05	0.09/0.09
ΔCA_{mean_tree} (m^2)	−1.50/−0.78	3.22/2.37	0.54/0.41	0.54/0.49
ΔCV_{mean_tree} (m^3)	−13.32/−3.75	46.12/58.08	12.99/14.92	8.15/10.53
ΔCSA_{mean_tree} (m^2)	−2.73/−1.50	23.89/29.74	9.44/9.41	4.39/5.57
ΔH_{mean_tree} (m)	0.02/−0.01	0.49/0.45	0.26/0.19	0.10/0.09
	Statistics of the mean values of Scots Pine/Norway spruce dominated sample plots (n = 44/24)			
ΔCD_{mean_plot} (m)	−0.03/−0.04	0.22/0.13	0.07/0.05	0.05/0.04
ΔCA_{mean_plot} (m^2)	−0.64/−0.11	2.06/0.97	0.54/0.40	0.39/0.29
ΔCV_{mean_plot} (m^3)	−1.15/2.26	27.66/26.42	13.60/14.87	5.76/6.86
ΔCSA_{mean_plot} (m^2)	0.73/2.50	16.03/17.30	9.48/9.26	2.91/3.65
ΔH_{mean_plot} (m)	0.06/0.09	0.46/0.38	0.25/0.18	0.10/0.08
	Statistics of the standard deviation values of Scots Pine/Norway spruce dominated sample plots (n = 38/21)			
ΔCD_{std_plot} (m)	0.01/0.01	0.24/0.15	0.08/0.08	0.04/0.04
ΔCA_{std_plot} (m^2)	0.11/0.14	1.87/0.93	0.46/0.41	0.32/0.20
ΔCV_{std_plot} (m^3)	2.15/2.34	16.09/16.89	6.98/7.98	3.33/4.39
ΔCSA_{std_plot} (m^3)	1.21/1.46	7.21/8.10	3.81/4.19	1.48/2.08
ΔH_{std_plot} (m)	0.01/0.01	0.09/0.10	0.04/0.04	0.02/0.02

2 m. These matched trees, along with their consecutive measurements, were then used to calculate the mean annual increments of tree height and crown dimensions (ΔH_{mean_tree}, ΔC_{mean_tree}) by dividing the observed change (T1 measurement subtracted from the respective T2 measurement) with the number of growing seasons in between the measurements. Table 4 summarizes these observations across the sampled trees.

Second, we established links between the ALS-derived trees and field-sampled trees to enable the assessment of how the obtained crown increments were associated with wood properties. The proximity of the geospatial locations between the ALS-derived and field-measured tree locations was utilized for this matching, aided by visual interpretation due to differing approaches for determining tree locations (tree top location for ALS compared to stem cross-section midpoint for field-sampling). This resulted in 257 Scots pine and 142 Norway spruce trees for tree-level analysis which were further used to calculate the plot-level means (ΔH_{mean_plot}, ΔC_{mean_plot}) and standard deviations (ΔH_{std_plot}, ΔC_{std_plot}) by tree species. Among the total number of 59 sample plots, Scots pine was represented by 44 sample plots and Norway spruce by 24 sample plots, and the plot-level means were computed for these sample plots. However, for assessing the standard deviations of wood properties, sample plots with at least three observations per species were considered, leaving 38 sample plots for Scots pine and 21 sample plots for Norway spruces. Table 4 summarizes these observations across the sample plots.

2.5. Statistical analysis

The relationships between wood properties and ALS-derived mean annual increments in tree height and crown dimensions were assessed by tree species due to assumed differences in the growth strategies between Scots pine and Norway spruce. We used Pearson's correlation coefficient (r) as a measure of the strength of the observed relationships. The correlations were considered to provide statistical support for the possible associations if the related p-values were < 0.05. The analyses were first conducted at the tree level, where a higher absolute value for r would imply a stronger association between wood properties (WD_{mean_tree}, RW_{mean_tree}) and mean annual increments in tree height and crown dimensions. This would allow us to assess the feasibility of utilizing ALS-derived metrics for monitoring the WD and RW of individual trees.

Then, we scaled up our analysis from tree-level to plot-level, aiming to assess the feasibility of utilizing ALS-derived metrics for estimating mean wood properties and their variation within sample plots. Employing r, these relationships were assessed between 1) averaged mean annual increments in tree height and crown dimensions and averaged mean wood properties (WD_{mean_plot} and RW_{mean_plot}) as well as 2) standard deviations in mean annual increments in tree height and crown dimensions and standard deviations in mean wood properties (WD_{std_plot} and RW_{std_plot}). Here, a higher absolute value for r would imply a stronger association between the investigated metrics, suggesting the feasibility of utilizing ALS for monitoring WD and RW of sample plots.

After obtaining insights into the possible associations, we modeled these relationships to assess the combined effects of studied metrics on mean wood properties at levels of the tree (WD_{mean_tree} and RW_{mean_tree}) and plot (WD_{mean_plot} and RW_{mean_plot}). A linear mixed-effect regression (LMER) was applied for the tree-level modeling to account for the possible variability in the associations between sample plots, in terms of their magnitude and direction, which could differ depending on site conditions that were not specified in this study. We conducted this analysis using the LME4 package in R software (Eq. 1) (Bates et al., 2015).

$$y_{ij} = \beta_0 + \beta_1 x_{1ij} + \beta_2 x_{2ij} + \ldots \beta_n x_{nij} + b_{0i} + \varepsilon_{ij} \quad (1)$$

where $y_{ij}$is the response variable of interest (WD_{mean_tree} or RW_{mean_tree}) for tree j within a sample plot i, $x_{1ij},\ldots,x_{nij}$ represent the fixed effects variables and β_0, $\beta_1,\ldots,\beta_n$ are corresponding coefficients. The b_{0i} and ε_{ij}

Table 5
Pearson's correlation coefficients and related statistical significance (p-value) measuring the relationships of tree-level basal area-weighted mean wood density (WD_{mean_tree}) and mean ring width (RW_{mean_tree}) with the respective ALS-derived mean annual increments of tree height (ΔH_{mean_tree}) and crown dimensions (ΔC_{mean_tree}) which were measured between T1 (2009) and T2 (2023). ΔH and ΔC stand for mean annual increment in tree height (H) and crown dimensions of diameter (CD), projection area (CA), volume (CV), and surface area (CSA). The level of significance is denoted as ^{ns} (not significant) for p-values > 0.05, * for p-value < 0.05, ** for p-value < 0.01, and *** for p-value < 0.001.

	Tree-level correlations of Scots Pine (n = 257)		Tree-level correlations of Norway spruce (n = 142)	
	WD_{mean_tree}			
	Correlation	p-value	Correlation	p-value
ΔCD_{mean_tree}	−0.02	0.707 ^{ns}	0.00	0.957 ^{ns}
ΔCA_{mean_tree}	−0.05	0.441 ^{ns}	0.02	0.789 ^{ns}
ΔCV_{mean_tree}	−0.04	0.560 ^{ns}	0.08	0.354 ^{ns}
ΔCSA_{mean_tree}	0.06	0.303 ^{ns}	0.06	0.444 ^{ns}
ΔH_{mean_tree}	0.08	0.220 ^{ns}	−0.17	0.039 *
	RW_{mean_tree}			
	Correlation	p-value	Correlation	p-value
ΔCD_{mean_tree}	0.14	0.029 *	−0.01	0.911 ^{ns}
ΔCA_{mean_tree}	0.21	< 0.001 ***	−0.01	0.921 ^{ns}
ΔCV_{mean_tree}	0.17	0.008 **	−0.03	0.685 ^{ns}
ΔCSA_{mean_tree}	0.16	0.012 *	−0.02	0.806 ^{ns}
ΔH_{mean_tree}	0.44	< 0.001 ***	0.43	< 0.001 **

denoted as normally distributed random effect for plot i and residual error, respectively with mean zero and unknown, unrestricted variance–covariance matrix. It is worth mentioning that fixed-effect variables were scaled into the range 0–1 using the min-max method to compare their contribution to the model. The MuMIn package of R was used to carry the information-theoretical model selection based on AIC (Akaike Information Criterion) (Barton, 2015). We tested models with different combinations of up to five predictors for both tree species and selected the ones with the lowest AIC for predicting $RW_{mean\text{-}ree}$ and $WD_{mean\text{-}tree}$. These models were assessed using the marginal coefficients of determination which account for the variance of fixed effects alone (R^2_m) and conditional coefficient of determination to consider the proportion of variance explained by both fixed and random effects (R^2_c).

At the plot-level, multiple linear regression was applied to investigate possible interaction between the ALS-derived plot-level variables in explaining variation in WD_{mean_plot} and RW_{mean_plot} employing the Stat package of R software (R Core Team, 2021). The model selection was carried out using a similar systematic approach as LMER. The adjusted R^2 (R^2_{adj}) was reported to measure the proportion of variance in WD_{mean_plot} and RW_{mean_plot} which was explained by the respective ALS-derived plot-level metrics.

3. Results

3.1. Relationship between the individual tree-level wood properties and the mean annual increments of tree height (ΔH_{mean_tree}) and crown dimensions (ΔC_{mean_tree})

The relationships between WD_{mean_tree}, RW_{mean_tree}, and ΔC_{mean_tree} measured by Pearson's correlation coefficients are presented in Table 5. We found none of the investigated ALS-derived metrics to correlate with WD_{mean_tree} of Scot pine (p-value > 0.05). ΔH_{mean_tree} was found as the

Table 6
Pearson's correlation coefficients and related statistical significance (p-values) measuring the relationships of plot level means and standard deviations of basal area-weighted mean wood density (WD_{mean_plot}, WD_{std_plot}) and mean ring width (RW_{mean_plot}, RW_{std_plot}) with the respective ALS-derived means and standard deviations of mean annual increments in tree height (ΔH_{mean_plot}, ΔH_{std_plot}) and crown dimensions (ΔC_{mean_plot}, ΔC_{std_plot}) measured between T1 (2009) and T2 (2023). ΔH and ΔC stand for annual increment in tree height (H) and crown dimensions of diameter (CD), projection area (CA), volume (CV), and surface area (CSA). The level of significance is denoted as ^{ns} (not significant) for p-values > 0.05, * for p-value < 0.05, ** for p-value < 0.01, and *** for p-value < 0.001.

	Plot-level correlations of mean values of Scots Pines (n = 44)				Plot-level correlations of mean values of Norway spruce (n = 24)			
	WD_{mean_plot}		RW_{mean_plot}		WD_{mean_plot}		RW_{mean_plot}	
	Correlation	p-value	Correlation	p-value	Correlation	p-value	Correlation	p-value
ΔCD_{mean_plot}	0.10	0.538 ^{ns}	0.02	0.893 ^{ns}	−0.01	0.972 ^{ns}	−0.16	0.457 ^{ns}
ΔCA_{mean_plot}	0.16	0.287 ^{ns}	0.01	0.972 ^{ns}	0.24	0.255 ^{ns}	−0.25	0.246 ^{ns}
ΔCV_{mean_plot}	0.14	0.363 ^{ns}	−0.12	0.448 ^{ns}	0.27	0.200 ^{ns}	−0.34	0.104 ^{ns}
ΔCSA_{mean_plot}	0.36	0.01 *	−0.10	0.937 ^{ns}	0.19	0.364 ^{ns}	−0.25	0.241 ^{ns}
ΔCH_{mean_plot}	0.27	0.08 ^{ns}	0.48	< 0.001 ***	−0.30	0.153 ^{ns}	0.47	0.021 *
	Plot-level correlations of standard deviation values of Scots pine (n = 38)				Plot-level correlations of standard deviation values of Norway spruce (n = 21)			
	WD_{std_plot}		RW_{std_plot}		WD_{std_plot}		RW_{std_plot}	
	Correlation	p-value	Correlation	p-value	Correlation	p-value	Correlation	p-value
ΔCD_{std_plot}	0.13	0.440 ^{ns}	0.19	0.246 ^{ns}	−0.22	0.331 ^{ns}	0.35	0.124 ^{ns}
ΔCA_{std_plot}	0.19	0.257 ^{ns}	−0.03	0.843 ^{ns}	−0.37	0.103 ^{ns}	0.19	0.414 ^{ns}
ΔCV_{std_plot}	0.21	0.203 ^{ns}	0.02	0.896 ^{ns}	−0.15	0.514 ^{ns}	0.07	0.767 ^{ns}
ΔCSA_{std_plot}	0.15	0.374 ^{ns}	−0.01	0.947 ^{ns}	−0.23	0.324 ^{ns}	0.12	0.608 ^{ns}
ΔCH_{std_plot}	−0.20	0.236 ^{ns}	0.24	0.147 ^{ns}	−0.13	0.581 ^{ns}	0.25	0.283 ^{ns}

Table 7
The coefficient estimates, standard errors, and *p*-values for the models predicting basal area-weighted mean wood density and mean ring width measured between T1 (2009) and T2 (2023) at the levels of the individual tree (WD_{mean_tree}, RW_{mean_tree}) and plot (WD_{mean_plot}, RW_{mean_plot}). The level of significance is denoted as ^{ns} (not significant) for *p*-values > 0.05, * for *p*-value < 0.05, ** for *p*-value < 0.01, and *** for *p*-value < 0.001.

	Model parameters		Coefficient estimate	Standard Error	*p*-value	Coefficient estimate	Standard Error	*p*-value
			WD_{mean_tree}			RW_{mean_tree}		
Tree-level	Scots Pine (n = 257)	Intercept	0.55	0.01	2e−16 ***	0.42	0.13	0.002 **
		ΔCV_{mean_tree}	−0.18	0.06	0.003 **	2.39	0.57	< 0.001 ***
		ΔCSA_{mean_tree}	0.15	0.05	0.003 **	−1.57	0.49	0.002 **
		ΔH_{mean_tree}	-	-	-	0.99	0.17	< 0.001 ***
	Norway spruce (n = 142)	Intercept	0.46	0.01	2e−16 ***	0.77	0.12	< 0.001 ***
		ΔH_{mean_tree}	-	-	-	1.20	0.27	< 0.001 ***
			WD_{mean_plot}			RW_{mean_plot}		
Plot-level	Scots pine (n = 44)	Intercept	0.50	0.01	2e−16 ***	0.90	0.11	3.58e−10 ***
		ΔH_{mean_plot}	-	-	-	0.73	0.20	< 0.001 ***
		ΔCSA_{mean_plot}	0.06	0.02	0.01 *	-	-	-
	Norway spruce (n = 24)	Intercept	0.46	0.01	2e−16 ***	1.02	0.11	8.56e−09 ***
		ΔH_{mean_plot}	-	-	-	0.71	0.28	0.02 *

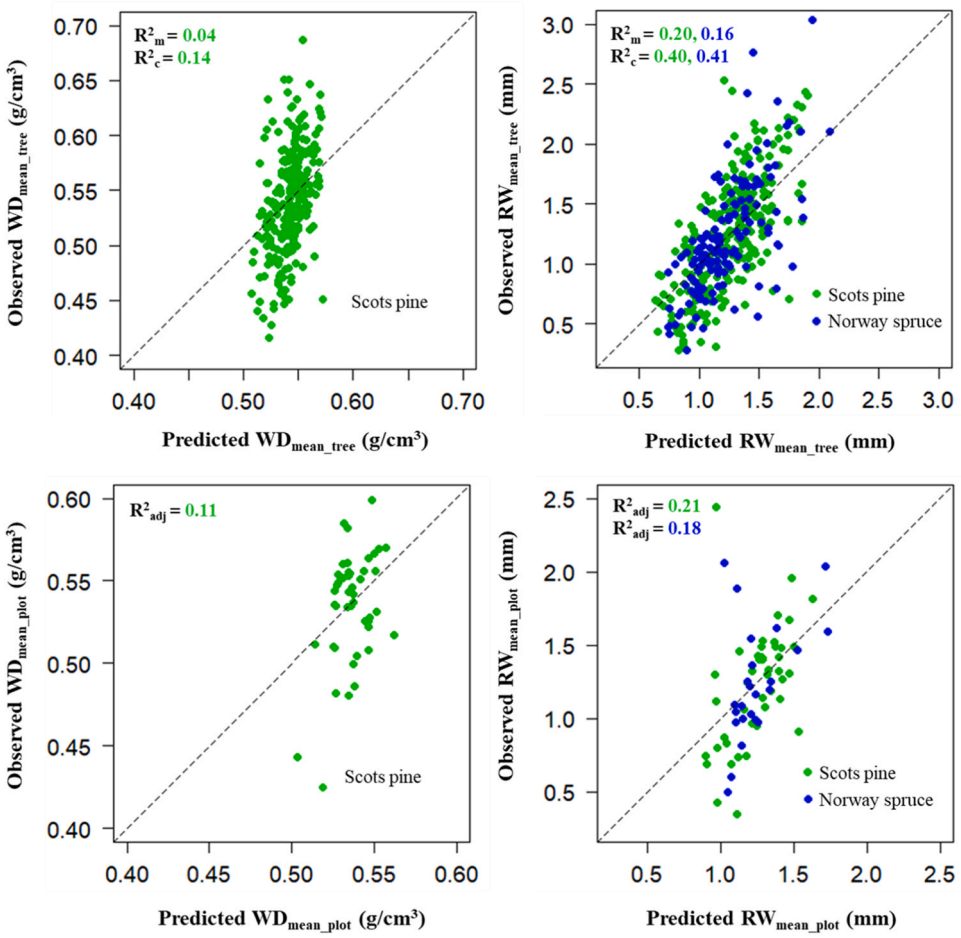

Fig. 4. Scatter plots of observed versus predicted basal area-weighted mean wood density and mean ring width measured between T1 (2009) and T2 (2023) at the levels of the individual tree (WD_{mean_tree}, RW_{mean_tree}) and plot (WD_{mean_plot}, RW_{mean_plot}). The dashed line represents a 1:1 relationship.

only ALS-derived metric that showed a statistically significant correlation with WD_{mean_tree} of Norway spruces (r = -0.17, *p*-value < 0.05). The observed associations were stronger for RW_{mean_tree}, where ΔH_{mean_tree} demonstrated the highest correlations regardless of tree species (r = 0.43–0.43). For Scots pine, ΔCA_{mean_tree} (r = 0.21) and ΔCV_{mean_tree} (r = 0.17) also showed rather weak but still statistically significant correlations with RW_{mean_tree} (*p*-value < 0.01). These positive correlations indicate that an increased mean annual increment in tree height and crown dimensions would be associated with an increased RW_{mean_tree}.

3.2. Relationship between the plot-level wood properties and the means and standard deviations of mean annual increments of tree height (ΔH_{mean_plot} and ΔH_{std_plot}) and crown dimensions (ΔC_{mean_plot} and ΔC_{std_plot})

Relationships between the plot-level wood properties and their respective ALS-derived mean annual increments in tree height and crown dimensions have been provided in Table 6. ΔCH_{mean_plot} was the only metric significantly related to RW_{mean_plot} regardless of tree species ($r = 0.47$–0.48). Considering WD_{mean_plot}, ΔCSA_{mean_plot} was the only metric showing a significant relationship ($r = 0.36$) for Scots pine. However, none of the metrics were significantly associated with the WD_{mean_plot} of Norway spruces. Weak correlations were recorded for the plot-level standard deviation of wood properties and respective ALS-derived metrics, but the associations were not statistically significant (p-value > 0.05) (Table 6).

3.3. Assessing the wood properties at individual tree and plot levels

The models employing increments in tree height and crown dimensions for describing the variation in the tree-level WD_{mean_tree} and RW_{mean_tree} as well as plot-level WD_{mean_plot} and RW_{mean_plot} are provided in Table 7. According to LMER, WD_{mean_tree} of Scots pine seemed to be associated with ΔCV_{mean_tree} and ΔCSA_{mean_tree}. The model coefficients implied that a decreased ΔCV_{mean_tree} and an increased ΔCSA_{mean_tree} was associated with an increased WD_{mean_tree}. Considering these fixed effects, the model could explain only 4 % of the observed variation in WD_{mean_tree} ($R^2_m = 0.04$) while the inclusion of random effects to account for the variability between sample plots slightly improved the model performance ($R^2_c = 0.14$) (Fig. 4). Regarding Norway spruce, none of the ALS-derived metrics were considered statistically significant in explaining WD_{mean_tree}.

For the RW_{mean_tree} of Scots pine, the LMER analysis showed that increases in ΔCV_{mean_tree} and ΔH_{mean_tree} as well as a decrease in ΔCSA_{mean_tree} were associated with an increased RW_{mean_tree} (Table 7). With these fixed effects, the model could explain 20 % of the observed variation in RW_{mean_tree} while the inclusion of random effects to account for the variability between sample plots improved the model performance ($R^2_c = 0.40$) (Fig. 4). For Norway spruce, ΔH_{mean_tree} was the only variable that demonstrated a statistically significant coefficient estimate of 1.20 for RW_{mean_tree}, indicating a positive association. Similar to Scots pine, the inclusion of random effects to account for the variability between sample plots slightly improved the model performance from $R^2_m = 0.16$ to $R^2_c = 0.41$ (Fig. 4).

At the plot-level, the observed variation in WD_{mean_plot} of Scots pine was explained by variation in ΔCSA_{mean_plot} with an R^2_{adj} of 0.11 (Fig. 4). Instead, none of the ALS-derived metrics were considered statistically significant in explaining the WD_{mean_plot} of Norway spruce. However, the variation in ΔH_{mean_plot} was significantly associated with the variation in RW_{mean_plot} of both Scots pines and Norway spruces by a similar coefficient estimate of 0.71–0.73 (Table 7). This indicates that as the ΔH_{mean_plot} increases, the RW_{mean_plot} also tends to increase. Assessment of the model performances showed that ALS-derived ΔH_{mean_plot} could explain 21 % and 18 % of observed variations in RW_{mean_plot} of Scots pine and Norway spruces, respectively (Fig. 4).

4. Discussion

In this study, we investigated how mean annual increments in tree height and crown dimensions obtained with bi-temporal ALS data can be associated with wood properties measured by X-ray microdensitometry of different tree species (i.e. Scots pine and Norway spruce) at both tree and plot levels. When assessing the relationship at the tree-level, all the studied ALS metrics were correlated with the RW_{mean_tree} of Scot pines, whereas ΔH_{mean_tree} was the only metric correlated with WD_{mean_tree} and RW_{mean_tree} of Norway spruces (Table 5). There was no correlation between WD_{mean_tree} and ALS metrics for Scots pines at the tree-level. Similarly, ΔH_{mean_plot} correlated with the RW_{mean_plot} of both Scot pines and Norway spruces at the plot-level, but for Scots pines, there was also a correlation between WD_{mean_plot} and ΔCSA_{mean_plot} (Table 6). The significant correlations between increments in tree height and RW for both Scots pine and Norway spruce at the tree and plot levels are an indication of a relationship between tree height and diameter growth (assessed here through ring width). This was also supported by the results from mixed-effect and multiple linear regression modeling as increment in tree height, either at tree or plot level, was a significant predictor for all the models. This aligned with previous findings as tree height and its growth have been related to the stand density and radial growth (Valentine et al., 2012). However, there are also contrasting results in Kankare et al., (2022) as increment in height was not significantly correlated with RW when it was calculated by differencing TLS height from field-measured height. This difference between the studies could have been attributed to the enhanced tree height characterization capability of ALS due to the above-canopy viewpoint of ALS (e.g.Wang et al., 2019). It should be noted that while an increased height growth may indicate an overall enhanced growth rate of the tree, changes in wood density are primarily driven by alterations in radial growth, which affect the proportions of lower-density earlywood and higher-density latewood production (Timell, 1986). Since ALS cannot directly measure the thickening of stem and branches, increases in crown dimensions were expected to reflect conditions where radial growth might have occurred. This expectation is supported by previous studies that have demonstrated a link between crown structure and a tree's past radial growth (Pretzsch et al., 2022).

For Scots pine, there were also significant correlations between RW_{mean_tree} and increment in all the crown metrics of Scots pines at the tree-level. In particular, tree-level modeling showed ΔCSA_{mean_tree} and ΔCV_{mean_tree} as significant predictors (Table 7). This can be related to the relationship between RW as well as increment in both tree height and crown metrics due to the interplay between photosynthetic leaves and growth rate (Pretzsch et al., 2022). The model explaining Norway spruce RW at the tree-level, however, was not statistically significant. Contrasting results were obtained by Pretzsch et al. (2022) where they fitted a regression model explaining variation in the annual diameter growth of Norway spruce trees with TLS-derived crown characteristics within a mature monospecific stand. They found the standard deviation of the maximum crown radius along the stem axis and crown top-heaviness as significant metrics. In a similar study, Ahmed et al. (2024) showed a significant correlation between tree ring width and crown metrics such as the coefficient of variation of crown radius ($r = 0.68$) and crown length ($r = 0.77$) across Norway spruces. While their study consisted of four stand types that significantly contributed to the observed variability of crown shapes and ring patterns, this rather strong relationship is in contrast with the current study. It is worth mentioning that they utilized the intensive TLS scan and manual tree extraction which may have affected the results and could complicate the comparison to this study.

For RW_{mean_plot}, ΔCH_{mean_plot} was the only metric that showed a statistically significant correlation for both Scots pine and Norway spruce at the plot-level which was supported by the regression modeling as ΔCH_{mean_plot} was the only metric included in the models predicting RW_{mean_plot} for both tree species (Table 7).

Our results did not show statistically significant correlations between WD_{mean_tree} and mean annual increments in tree height and crown dimensions for Scots pines (Table 5). However, ΔCSA_{mean_tree} and ΔCV_{mean_tree} were included in the mixed-effect model for Scots pine as significant predictors when predicting WD_{mean_tree}. The results obtained by Kankare et al. (2022) were similar as they did not find statistical evidence for the initial tree height and crown metrics of width, area, volume, and length, as well as height increment to correlate with WD of Scots pine trees. Instead, they found the mean branch angle as a significant predictor to explain 31 % of the WD variation between trees. Pyörälä et al. (2019) also found moderate correlations of −0.49 and

−0.61 between X-ray-derived WD measurements and TLS-derived stem taper and volume for Scots pine trees, respectively. It should be noted that both of the above-mentioned studies only utilized one-time point TLS data and neither of them investigated the effects of changes in crown size on wood density. For Norway spruce, however, ΔH_{mean_tree} had a statistically significant, although rather low correlation with WD_{mean_tree} (Table 5) but no ALS metric was significant for predicting WD_{mean_tree} of Norway spruce (Table 7). It is worth mentioning that the study period investigated in the current study only focuses on the last 15 growing seasons corresponding with ALS acquisitions. This might limit the dependencies between crown development and wood density, particularly given the age of sample trees at an average of 64 years for Scots pine and 84 years for Norway spruces (Table 2). Wood density is mostly determined by tree age as a result of cambium maturation and thus it largely varies from corewood to outerwood (Wylie et al., 2019). Many of the studied trees were likely producing outerwood within this period considering their age. The high, stable wood density in the outerwood, driven by a high proportion of latewood, could diminish observed correlations. Additionally, the variation in wood density is more pronounced over a longer time frame as age-related changes in cambial activity occur gradually, particularly for older trees already in the outerwood production phase. However, other environmental factors such as resource availability, precipitation, and temperature in the growing season could have affected the annual variability in wood density along with tree age (Rocha et al., 2019). For Norway spruces, on the other hand, the latewood production is generally consistent, and earlywood tends to vary more in response to environmental factors. Nevertheless, up to 80 % of the variation in Norway spruce WD comes from differences within annual rings (Jyske et al., 2008), which were averaged out in our experimental design.

At the plot-level, the only significant correlation was found between ΔCSA_{mean_plot} and WD_{mean_plot} of Scots pines, suggesting that an increment in crown surface area increases the mean wood density (Table 6). Similarly, the ΔCSA_{mean_plot} was the only statistically significant predictor when predicting wood density at the plot-level (Table 7). For Norway spruce, none of the metrics showed a significant correlation or were significant predictors in the developed models. In comparison, Luther et al., (2014) explained 40–53 % of plot-level variations in fiber attributes such as density across the boreal forest of Canada dominated by balsam fir (*Abies balsamea* (L.) Mill) and black spruce (*Picea marana* (Mill.) Britton, Sterns and Poggenb) trees. They used ALS-derived parameters of height, density, and canopy complexity for predictions. However, several other factors such as environmental conditions and past management activities likely contributed to the variability in wood properties which was not fully captured by crown increments in our study. Saarinen et al., (2022) and Ahmed et al., (2024), for example, have demonstrated how crown size and shape vary between sample plots with different management histories. Thus, the used metrics may not be the primary drivers of plot-level wood properties for the studied species. This was also confirmed by the mixed-effect modeling where the inclusion of random effects to account for the variability in the tree-level associations between sample plots improved the explanatory power of the RW_{mean_tree} and WD_{mean_tree} models (Table 7). Similarly, when assessing the standard deviation of wood properties at the plot-level, none of the metrics were significantly correlated for either species (Table 6). This might be caused by the low variability in the WD_{mean_tree} as the sample trees were selected among the dominant trees.

Altogether, the experiments carried out in this study aimed to evaluate the feasibility of an approach where ALS-derived mean annual increments in tree height and crown dimensions are related to wood properties. This would enable a nondestructive assessment of characteristics typically measured by destructive sampling with limited geospatial coverage. However, the results presented here may have been influenced by the relatively short timeframe, especially considering the lifespan of boreal tree species. During this period, there may not have been sufficient variation in growth patterns, as reflected by crown characteristics, to fully explain the observed differences in wood properties among trees. Specifically, the observed variation in WD_{mean_tree} was relatively small within this predominantly managed forest which may have affected the observed relationships with increments in crown metrics. In this context, it is important to emphasize the extraction of ALS-derived crown metrics, given the applied data and processing methods. First, the point clouds featured different data acquisition setups, leading to varying point cloud densities, which particularly affected the level of detail in point cloud-based observations. This inconsistency in point cloud characteristics may have affected the ability of the bitemporal approach to capture growth-induced changes in the studied metrics (Van Leeuwen et al., 2011). Nevertheless, even the lower-density T1 ALS data, with 25 pts/m^2, was considered sufficient for reconstructing tree crowns, and tree-level growth analysis (Zhao et al., 2018). Second, potential errors in the mean annual increment observations could have arisen from the applied tree crown segmentation method, particularly due to its repetition over time. In this approach, crown boundaries were first determined based on the CHM, and individual tree point clouds were delineated accordingly to compute volumetric characteristics. While this method is applicable regardless of point cloud density, the drawback is that errors in crown delineation can result in larger errors in volumetric characteristics when two-dimensional polygons are applied in the delineation of three-dimensional crown structures, assuming vertical crown boundaries. This is especially evident in closed canopies, where determining the boundaries of mixed crowns becomes rather arbitrary. However, since the same methodology was applied for both T1 and T2 data, the observed changes are still expected to reflect growth-induced increments at the level of accuracy attainable with bitemporal ALS. Nevertheless, the underlying relationship between crown increments and wood properties could have been obscured.

5. Conclusion

Forest management and timber procurement could benefit from information on wood properties and their variation. We developed and tested an integrated approach combining bi-temporal airborne laser scanning and X-ray microdensitometry to assess wood properties. Tree crown and stem growth are structurally and functionally linked, and their development affects the wood formation process. With the increased availability of multitemporal ALS data, there is a potential to use increments in tree height and crown dimensions as proxies for stem growth and, consequently, assess wood properties. Thus, the core idea of the developed approach was to link tree growth measured from ALS data collected at two-time points to wood properties. However, the observed correlations over the 15 growing seasons were not strong, and the predictive models could not explain a large portion of the variation in wood properties. The strongest relationships were observed between ring width and ALS-derived tree height and crown growth. Further research could benefit from applying the same methodology over a longer observation period or in younger stands, where growth rate differences are likely to be more pronounced in wood properties.

CRediT authorship contribution statement

Ghasem Ronoud: Writing – review & editing, Investigation, Formal analysis. **Maryam Poorazimy:** Writing – original draft, Visualization, Software, Methodology, Investigation, Formal analysis, Conceptualization. **Mikko Vastaranta:** Writing – review & editing, Supervision, Resources, Project administration, Methodology, Funding acquisition, Conceptualization. **Ninni Saarinen:** Writing – review & editing, Supervision, Conceptualization. **Ville Kankare:** Writing – review & editing, Supervision, Conceptualization. **Tuomas Yrttimaa:** Writing – review & editing, Methodology, Conceptualization. **Juha Hyyppä:** Resources, Project administration, Funding acquisition.

Declaration of Competing Interest

The authors declare that they have no known competing financial interests or personal relationships that could have appeared to influence the work reported in this paper.

Acknowledgment

The authors would like to acknowledge financial support by the Research Council of Finland through Forest–Human–Machine Interplay flagship of science [decision number 337127], Density4Trees project [decision number 331711], and Scan4erstEcosystem Research Infrastructure [decision number 337810 and 346383]. Thanks also go to Jarmo Pennala, laboratory specialist at UEF School of Forest Sciences, for analyzing wood samples.

Data availability

Data will be made available on request.

References

Ahmed, S., Hilmers, T., Uhl, E., Jacobs, M., Bohnhorst, L., Kolisnyk, B., del Río, M., Pretzsch, H., 2024. Neighborhood competition modulates the link between crown structure and tree ring variability in monospecific and mixed forest stands. For. Ecol. Manag. 560. https://doi.org/10.1016/j.foreco.2024.121839.

Åkerblom, M., Kaitaniemi, P., 2021. Terrestrial laser scanning: A new standard of forest measuring and modelling. Ann. Bot. 128, 653–662. https://doi.org/10.1093/aob/mcab111.

Axelsson, P., 2000. DEM Generation from Laser Scanner Data Using adaptive TIN Models. Int. Arch. Photogramm. Remote Sens 23, 110–117.

Barton, K., 2015. Package "MuMIn" [WWW Document]. R Packag. version 1.15.1. URL https://cran.r-project.org/web/packages/MuMIn/MuMIn.pdf.

Bates, D., Mächler, M., Bolker, B.M., Walker, S.C., 2015. Fitting. Linear mixed-Eff. Models Using lme4. J. Stat. Softw. 67. https://doi.org/10.18637/jss.v067.i01.

Bergsten, U., Lindeberg, J., Rindby, A., Evans, R., 2001. Batch measurements of wood density on intact or prepared drill cores using x-ray microdensitometry. Wood Sci. Technol. 35, 435–452. https://doi.org/10.1007/s002260100106.

Biondi, F., Qeadan, F., 2008. A theory-driven approach to tree-ring standardization: Defining the biological trend from expected basal area increment. Tree-Ring Res 64, 81–96. https://doi.org/10.3959/2008-6.1.

Demol, M., Calders, K., Krishna Moorthy, S.M., Van den Bulcke, J., Verbeeck, H., Gielen, B., 2021. Consequences of vertical basic wood density variation on the estimation of aboveground biomass with terrestrial laser scanning. Trees - Struct. Funct. 35, 671–684. https://doi.org/10.1007/s00468-020-02067-7.

Downes, G.M., Drew, D.M., 2008. Climate and growth influences on wood formation and utilisation. South 70, 155–167. https://doi.org/10.2989/SOUTH.FOR.2008.70.2.11.539.

Duchesne, I., Wilhelmsson, L., Spangberg, K., 1997. Effects of in-forest sorting of Norway spruce (*Picea abies*) and Scots pine (*Pinus sylvestris*) on wood and fibre properties. Can. J. For. Res. 27, 790–795. https://doi.org/10.1139/x97-040.

Duncanson, L., Dubayah, R., 2018. Monitoring individual tree-based change with airborne lidar. Ecol. Evol. 8, 5079–5089. https://doi.org/10.1002/ece3.4075.

Fassnacht, F.E., White, J.C., Wulder, M.A., Næsset, E., 2024. Remote sensing in forestry: current challenges, considerations and directions. Forestry 97, 11–37. https://doi.org/10.1093/forestry/cpad024.

Frew, M.S., Evans, D.L., Londo, H.A., Cooke, W.H., Irby, D., 2016. Measuring douglas-fir crown growth with multitemporal LiDAR. For. Sci. 62, 200–212. https://doi.org/10.5849/forsci.14-062.

Genet, A., Auty, D., Achim, A., Bernier, M., Pothier, D., Cogliastro, A., 2013. Consequences of faster growth for wood density in nothern read oak (*Quercus rubra* Liebl.). For.: Int. J. For. Res. 86 (1), 99–110. https://doi.org/10.1093/forestry/cps057.

Hein, S., Weiskittel, A.R., Kohnle, U., 2008. Effect of wide spacing on tree growth, branch and sapwood properties of young Douglas-fir [*Pseudotsuga menziesii* (Mirb.) Franco] in south-western Germany. Eur. J. For. Res. 127, 481–493. https://doi.org/10.1007/s10342-008-0231-9.

Hyyppä, J., Hyyppä, H., Leckie, D., Gougeon, F., Yu, X., Maltamo, M., 2008. Review of methods of small-footprint airborne laser scanning for extracting forest inventory data in boreal forests. Int. J. Remote Sens. 29, 1339–1366. https://doi.org/10.1080/01431160701736489.

Ikonen, V.P., Peltola, H., Wilhelmsson, L., Kilpeläinen, A., Väisänen, H., Nuutinen, T., Kellomäki, S., 2008. Modelling the distribution of wood properties along the stems of Scots pine (*Pinus sylvestris* L.) and Norway spruce (*Picea abies* (L.) Karst.) as affected by silvicultural management. For. Ecol. Manag. 256, 1356–1371. https://doi.org/10.1016/j.foreco.2008.06.039.

Jevšenak, J., Klisz, M., Mašek, J., Čada, V., Janda, P., Svoboda, M., Vostarek, O., Treml, V., van der Maaten, E., Popa, A., Popa, I., van der Maaten-Theunissen, M., Zlatanov, T., Scharnweber, T., Ahlgrimm, S., Stolz, J., Sochová, I., Roibu, C.C., Pretzsch, H., Schmied, G., Uhl, E., Kaczka, R., Wrzesiński, P., Šenfeldr, M., Jakubowski, M., Tumajer, J., Wilmking, M., Obojes, N., Rybníček, M., Lévesque, M., Potapov, A., Basu, S., Stojanović, M., Stjepanović, S., Vitas, A., Arnič, D., Metslaid, S., Neycken, A., Prislan, P., Hartl, C., Ziche, D., Horáček, P., Krejza, J., Mikhailov, S., Světlík, J., Kalisty, A., Kolář, T., Lavnyy, V., Hordo, M., Oberhuber, W., Levanič, T., Mészáros, I., Schneider, L., Lehejček, J., Shetti, R., Bošeľa, M., Copini, P., Koprowski, M., Sass-Klaassen, U., Izmir, Ş.C., Bakys, R., Entner, H., Esper, J., Janecka, K., Martinez del Castillo, E., Verbylaite, R., Árvai, M., de Sauvage, J.C., Čufar, K., Finner, M., Hilmers, T., Kern, Z., Novak, K., Ponjarac, R., Puchałka, R., Schuldt, B., Škrk Dolar, N., Tanovski, V., Zang, C., Žmegač, A., Kuithan, C., Metslaid, M., Thurm, E., Hafner, P., Krajnc, L., Bernabei, M., Bojić, S., Brus, R., Burger, A., D'Andrea, E., Đorem, T., Gławęda, M., Gričar, J., Gutalj, M., Horváth, E., Kostić, S., Matović, B., Merela, M., Miletić, B., Morgós, A., Paluch, R., Pilch, K., Rezaie, N., Rieder, J., Schwab, N., Sewerniak, P., Stojanović, D., Ullmann, T., Waszak, N., Zin, E., Skudnik, M., Oštir, K., Rammig, A., Buras, A., 2024. Incorporating high-resolution climate, remote sensing and topographic data to map annual forest growth in central and eastern Europe. Sci. Total Environ. 913. https://doi.org/10.1016/j.scitotenv.2023.169692.

Jyske, T., Mäkinen, H., Saranpää, P., 2008. Wood density within Norway spruce stems. Silva Fenn. 42, 439–455. https://doi.org/10.14214/sf.248.

Kankare, V., Saarinen, N., Pyörälä, J., Yrttimaa, T., Hynynen, J., Huuskonen, S., Hyyppä, J., Vastaranta, M., 2022. Assessing the Dependencies of Scots Pine (*Pinus sylvestris* L.) Structural Characteristics and Internal Wood Property Variation. Forests 13. https://doi.org/10.3390/f13030397.

Kankare, V., Vauhkonen, J., Tanhuanpää, T., Holopainen, M., Vastaranta, M., Joensuu, M., Krooks, A., Hyyppä, J., Hyyppä, H., Alho, P., et al., 2014. Accuracy in estimation of timber assortments and stem distribution–A comparison of airborne and terrestrial laser scanning techniques. ISPRS J. Photogramm. Remote Sens. 97, 89–97.

Khosravipour, A., Skidmore, A.K., Isenburg, M., 2016. Generating spike-free digital surface models using LiDAR raw point clouds: A new approach for forestry applications. Int. J. Appl. Earth Obs. Geoinf. 52, 104–114. https://doi.org/10.1016/j.jag.2016.06.005.

Krajnc, L., Farrelly, N., Harte, A.M., 2019. The influence of crown and stem characteristics on timber quality in softwoods. For. Ecol. Manag. 435, 8–17. https://doi.org/10.1016/j.foreco.2018.12.043.

Kuprevicius, A., Auty, D., Achim, A., Caspersen, J.P., 2013. Quantifying the influence of live crown ratio on the mechanical properties of clear wood. Forestry 86, 361–369. https://doi.org/10.1093/forestry/cpt006.

Larson, P., 1969. Wood formation and the concept of wood quality. Yale Univ. Sch. For. Bull. 1–54.

Liang, X., Kankare, V., Hyyppä, J., Wang, Y., Kukko, A., Haggrén, H., Yu, X., Kaartinen, H., Jaakkola, A., Guan, F., et al., 2016. Terrestrial laser scanning in forest inventories. ISPRS J. Photogramm. Remote Sens 115, 63–77.

Luoma, V., Yrttimaa, T., Kankare, V., Saarinen, N., Pyörälä, J., Kukko, A., Kaartinen, H., Hyyppä, J., Holopainen, M., Vastaranta, M., 2021. Revealing changes in the stem form and volume allocation in diverse boreal forests using two-date terrestrial laser scanning. Forests 12, 835.

Luther, J.E., Skinner, R., Fournier, R.A., Van Lier, O.R., Bowers, W.W., Coté, J.F., Hopkinson, C., Moulton, T., 2014. Predicting wood quantity and quality attributes of balsam fir and black spruce using airborne laser scanner data. Forestry 87, 313–326. https://doi.org/10.1093/forestry/cpt039.

Ma, Q., Su, Y., Tao, S., Guo, Q., 2018. Quantifying individual tree growth and tree competition using bi-temporal airborne laser scanning data: a case study in the Sierra Nevada Mountains, California. Int. J. Digit. Earth 11, 485–503. https://doi.org/10.1080/17538947.2017.1336578.

Mäkinen, H., Colin, F., 1998. Predicting branch angle and branch diameter of Scots pine from usual tree measurements and stand structural information. Can. J. For. Res 28, 1686–1696. https://doi.org/10.1139/cjfr-28-11-1686.

Meyer, F., Beucher, S., 1990. Morphological segmentation. J. Vis. Commun. Image Represent 1, 21–46. https://doi.org/10.1016/1047-3203(90)90014-M.

Peltola, H., Kilpeläinen, A., Sauvala, K., Räisänen, T., Ikonen, V.P., 2007. Effects of early thinning regime and tree status on the radial growth and wood density of scots pine. Silva Fenn. 41, 489–505. https://doi.org/10.14214/sf.285.

Pokharel, B., Groot, A., Pitt, D.G., Woods, M., Dech, J.P., 2016. Predictive modeling of black spruce (*Picea mariana* (Mill.) B.S.P.) wood density using stand structure variables derived from airborne LiDAR data in boreal forests of Ontario. Forests 7 https://doi.org/10.3390/f7120311.

Poorazimy, M., Ronoud, G., Yrttimaa, T., Hyyppä, J., Saarinen, N., Kankare, V., Vastaranta, M., 2024. Understanding the species-specific tree growth dependencies using close-range multisensorial point clouds. Submitted. to Eur. J. For. Res.

Poorazimy, M., Ronoud, G., Yu, X., Luoma, V., Hyyppä, J., Saarinen, N., Kankare, V., Vastaranta, M., 2022. Feasibility of Bi-Temporal Airborne Laser Scanning Data in Detecting Species-Specific Individual Tree Crown Growth of Boreal Forests. Remote Sens 14. https://doi.org/10.3390/rs14194845.

Pretzsch, H., 2021. Tree growth as affected by stem and crown structure. Trees - Struct. Funct. 35, 947–960. https://doi.org/10.1007/s00468-021-02092-0.

Pretzsch, H., Ahmed, S., Jacobs, M., Schmied, G., Hilmers, T., 2022. Linking crown structure with tree ring pattern: methodological considerations and proof of concept. Trees - Struct. Funct. 36, 1349–1367. https://doi.org/10.1007/s00468-022-02297-x.

Pyörälä, J., Kankare, V., Liang, X., Saarinen, N., Rikala, J., Kivinen, V.P., Sipi, M., Holopainen, M., Hyyppä, J., Vastaranta, M., 2019. Assessing log geometry and wood quality in standing timber using terrestrial laser-scanning point clouds. Forestry 92, 177–187. https://doi.org/10.1093/forestry/cpy044.

R Core Team, 2021. A language and environment for statistical computing. R Found. Stat. Comput.

Raumonen, P., Kaasalainen, M., Markku, Å., Kaasalainen, S., Kaartinen, H., Vastaranta, M., Holopainen, M., Disney, M., Lewis, P., 2013. Fast automatic precision tree models from terrestrial laser scanner data. Remote Sens 5, 491–520. https://doi.org/10.3390/rs5020491.

Rocha, M.F.V., Veiga, T.R.L.A., Soares, B.C.D., de Araújo, A.C.C., Carvalho, A.M.M., Hein, P.R.G., 2019. Do the growing conditions of trees influence the wood properties? Floresta e Ambient 26. https://doi.org/10.1590/2179-8087.035318.

Saarinen, N., Kankare, V., Huuskonen, S., Hynynen, J., Bianchi, S., Yrttimaa, T., Luoma, V., Junttila, S., Holopainen, M., Hyyppä, J., Vastaranta, M., 2022. Effects of Stem Density on Crown Architecture of Scots Pine Trees. Front. Plant Sci. 13. https://doi.org/10.3389/fpls.2022.817792.

Schimleck, L., Dahlen, J., Apiolaza, L.A., Downes, G., Emms, G., Evans, R., Moore, J., Pâques, L., Van den Bulcke, J., Wang, X., 2019. Non-destructive evaluation techniques and what they tell us about wood property variation. Forests 10. https://doi.org/10.3390/f10090728.

Seidel, D., Schall, P., Gille, M., Ammer, C., 2015. Relationship between tree growth and physical dimensions of Fagus sylvatica crowns assessed from terrestrial laser scanning. iForest - Biogeosciences 8, 735. https://doi.org/10.3832/IFOR1566-008.

Timell, T.E., 1986. Compression Wood in Gymnosperms. Compress. Wood Gymnosperms. https://doi.org/10.1007/978-3-642-61616-7.

Valentine, H.T., Mäkelä, A., Green, E.J., Amateis, R.L., Mäkinen, H., Ducey, M.J., 2012. Models relating stem growth to crown length dynamics: Application to loblolly pine and Norway spruce. Trees - Struct. Funct. 26, 469–478. https://doi.org/10.1007/S00468-011-0608-0/FIGURES/7.

Van Leeuwen, M., Hilker, T., Coops, N.C., Frazer, G., Wulder, M.A., Newnham, G.J., Culvenor, D.S., 2011. Assessment of standing wood and fiber quality using ground and airborne laser scanning: A review. For. Ecol. Manag. 261, 1467–1478. https://doi.org/10.1016/j.foreco.2011.01.032.

Wang, Y., Lehtomäki, M., Liang, X., Pyörälä, J., Kukko, A., Jaakkola, A., Liu, J., Feng, Z., Chen, R., Hyyppä, J., 2019. Is field-measured tree height as reliable as believed – A comparison study of tree height estimates from field measurement, airborne laser scanning and terrestrial laser scanning in a boreal forest. ISPRS J. Photogramm. Remote Sens 147, 132–145. https://doi.org/10.1016/j.isprsjprs.2018.11.008.

White, J.C., Coops, N.C., Wulder, M.A., Vastaranta, M., Hilker, T., Tompalski, P., 2016. Remote Sensing Technologies for Enhancing Forest Inventories: A Review. Can. J. Remote Sens. 42, 619–641. https://doi.org/10.1080/07038992.2016.1207484.

White, J.C., Tompalski, P., Vastaranta, M., Wulder, M.A., Saarinen, S., Stepper, C., Coops, N.C., 2017. A model development and application guide for generating an enhanced forest inventory using airborne laser scanning data and an area-based approach. In: CWFC Information Report FI-X-018, Canadian Forest Service. Pacific Forestry Centre, Victoria, BC, Canada, p. 38.

Wylie, R.R.M., Woods, M.E., Dech, J.P., 2019. Estimating stand age from airborne laser scanning data to improve models of black spruce wood density in the boreal forest of Ontario. Remote Sens 11. https://doi.org/10.3390/rs11172022.

Yrttimaa, T., Junttila, S., Luoma, V., Calders, K., Kankare, V., Saarinen, N., Kukko, A., Holopainen, M., Hyyppä, J., Vastaranta, M., 2023. Capturing seasonal radial growth of boreal trees with terrestrial laser scanning. For. Ecol. Manag. 529. https://doi.org/10.1016/j.foreco.2022.120733.

Yrttimaa, T., Luoma, V., Saarinen, N., Kankare, V., Junttila, S., Holopainen, M., Hyyppä, J., Vastaranta, M., 2022. Exploring tree growth allometry using two-date terrestrial laser scanning. For. Ecol. Manag. 518, 120303. https://doi.org/10.1016/J.FORECO.2022.120303.

Zeller, L., Ammer, C., Annighöfer, P., Biber, P., Marshall, J., Schütze, G., del Río Gaztelurrutia, M., Pretzsch, H., 2017. Tree ring wood density of Scots pine and Europaen beech lower in mixed-speccies stands compared with monocultures. For. Ecol. Manag. 400, 363–374. https://doi.org/10.1016/j.foreco.2017.06.018.

Zhao, K., Suarez, J.C., Garcia, M., Hu, T., Wang, C., Londo, A., 2018. Utility of multitemporal lidar for forest and carbon monitoring: Tree growth, biomass dynamics, and carbon flux. Remote Sens. Environ. 204, 883–897. https://doi.org/10.1016/j.rse.2017.09.007.